Electrical Power and Energy Systems 62 (2014) 679–688

Contents lists available at ScienceDirect

Electrical Power and Energy Systems

journal homepage: www.elsevier.com/locate/ijepes

Vulnerability assessment and reconfiguration of microgrid through search vector artificial physics optimization algorithm

Xin Zhan, Tieyuan Xiang *, Hongkun Chen, Bo Zhou, Zaihe Yang

Department of Electrical Engineering, Wuhan University at Wuhan, Hubei Province, China

ARTICLE INFO

Article history:
Received 4 July 2013
Received in revised form 21 April 2014
Accepted 13 May 2014

Keywords:
Microgrid
Structure vulnerability
Comprehensive sensitivity
Vulnerability assessment system
Reconfiguration
SVAPO

ABSTRACT

Taking the mathematical model and reliability parameters of the microgrid into account, this paper has proposed two vulnerability assessment indices (VAI) – weighted complex network structure parameters and comprehensive operational sensitivity to set up a vulnerability assessment system. The microgrid reconfiguration (MR) model is built with consideration of the grid-connected/island mode and the VAI. A novel artificial physics optimization algorithm with a searching vector (SVAPO) is presented and applied to minimize the system vulnerability. The technique has been successfully implemented on CERTS and 38-bus microgrids to demonstrate the performance and effectiveness of the proposed method. The results obtained are encouraging.

Introduction

Microgrid reconfiguration (MR) is aimed at optimizing the network operation on the premise of meeting the basic requirement of the bus voltage, feeder current as well as configuration of radial network [1]. This paper addresses the purpose of achieving high power quality of sensitive loads, improving the bus voltage profile, and eliminating the overloads by adjusting the loads (including interruptible loads and adjustable loads) and changing the open/close status of sectionalizing switches, tie switches and the PCC switch in the system.

A microgrid can be regarded as a supplement to the large power grid, which is capable of improving the reliability and quality of power supply. Because of its inherent vulnerability [2], the vulnerability assessment of microgrid aims at finding out the weak points to enhance the system security and stability in order to guide the MR later in terms of reducing loss, load balancing and power restoration.

Microgrids are governed by droop control algorithms so they can operate in an autonomous fashion. Conventionally, Lasseter et al. [3] have suggested the real power–frequency droop control and the reactive power–voltage magnitude droop as the control strategies. In [4], a $Q - \dot{V}$ droop control method with $\dot{V}$ restoration mechanism is proposed to improve reactive power sharing. Rowe et al. [5] have introduced the concept of utilizing an arctan function for the power–frequency droop profile in a microgrid. Babazadeh and Karimi [6] have presented a new robust control strategy characterized by a two-degree-of-freedom feedback–feedforward controller for an islanded microgrid.

Most researches about vulnerability assessment only focus on the transmission network. In [7], a transmission vulnerability assessment method based on the fault chain theory of security science is proposed. The technique describes the cascading failure process and its generic features according to a fault chain. In [8], Ten et al. have presented a vulnerability assessment framework to systematically evaluate the vulnerabilities of SCADA systems. The proposed method is based on cyber systems embedded with the firewall and password models. Carrión et al. [9] have suggested network planners to select the new lines accounting for the vulnerability of the transmission network. The vulnerability of the transmission network is measured in terms of the expected load shed. In [10] Yu et al. have used adequacy indices, the security index probability of stability and integrated system vulnerability as VAI. Overbye and DeMarco [11] defined a security measure to indicate vulnerability based on an energy function for system models. In [12], Fouad et al. have presented the transient energy as a tool of analysis. Chen et al. [13] proposed a novel method using the line betweenness as the vulnerability index according to the complex network theory. In [14], Ying Shao and Jilai Yu have presented another new method for vulnerability assessment based on electrical dissection information.

* Corresponding author. Tel.: +86 15927332132.
E-mail address: xty01@163.com (T. Xiang).

http://dx.doi.org/10.1016/j.ijepes.2014.05.024
0142-0615/© 2014 The Authors. Published by Elsevier Ltd.

Notations

PCC	point of common coupling
V^*	nominal voltage set point
m_{pi}, n_{qi}	active and reactive power static gain of ith DG
P_{Gi}, Q_{Gi}	three-phase injected active power of ith DG
ω_i	output voltage frequency of ith DG
ω^*	nominal frequency set point
P_{Oi}, Q_{Oi}	nominal active and reactive power of load i
α, β	active and reactive power exponents
P_{Li}, Q_{Li}	active and reactive power of load i
P_i^a, Q_i^a	a phase active and reactive power at bus i
R_i	resistance at line i
γ_{os}	failure time probability of network topology
V_s	vulnerability value of structure indices
V_o	vulnerability value of operation indices
w_1, w_2, w_3	weighted value of each operation index
ISV_i	vulnerability value of element i
ISV	vulnerability value of the whole microgrid
NB	number of buses
V_i	voltage magnitude at bus i
V_i^{sp}	specified voltage magnitude at busi
$\Delta V_i^{\lim}$	voltage deviation limit
NL	number of lines
p_{li}	real power flow at line i
$p_{li}^{\lim}$	capacity of the line
$sevf_i$	frequency deviation judgment index
X_i	feeder switch at line i
X_{PCC}	PCC switch
A	incidence matrix of node-line
P	vector of power flow
V_o^{sp}	nominal deviation set of operation indices
D	vector of load demand
g_k	set of current configuration
G_k	set of radial configuration
N	operation numbers of switch
$N_{\max}$	maximum switching numbers allowed
x_{best}, x_{worst}	the position of best and worst adaptive value
$v_{i,k}$	speed vector of individual i in kth dimension
$x_{i,k}$	position vector of individual i in kth dimension
G	gravitational constant
w	inertia weight factor
λ	random number between 0 and 1
x_k^u	upper limit of position vector in kth dimension
x_k^l	lower limit of position vector in kth dimension

Traditionally, the main objective of reconfiguration is dedicated to minimize the total power loss. Due to the uniqueness of microgrids, the conventional distribution system reconfiguration is not totally suitable for the MR. In addition, much research are only conducted on distribution system. Gonzáleza et al. [15] proposed a method for computing the sensitivities of the state variables with respect to switching operations and obtaining estimations of voltages and power flow in the network. In [16], Srinivasa Rao et al. have presented a new method to solve the network reconfiguration problem in the presence of DG with an objective of minimizing real power loss and improving voltage profile in distribution system. A meta heuristic Harmony Search Algorithm (HSA) is used to simultaneously reconfigure. Zin et al. [17] have put forward a new heuristic method to optimize the network based on minimum branch current in the system. Malekpour et al. [18] made a significant contribution to interactive fuzzy satisfying optimization algorithm based on adaptive particle swarm optimization (APSO) for the optimal reconfiguration plan. In [19], Zin et al. have developed two hybrid heuristic methods for reconfiguration of the radial electrical distribution system. A circular minimum branch-current updating mechanism is proposed to pass the local optimum points. Then, the best known configuration is obtained according to a circular neighbor-chain updating technique.

This paper analyzes the network characteristics with the complex network theory on the basis of the mathematical model and power flow calculation of microgrid. Considering the reliability and operational sensitivity of the bus and feeder, the vulnerability assessment system of microgrid is proposed on the purpose of the energy demand management and power quality for users. The reconfiguration model aiming at minimum the total vulnerability value is built. The algorithm is tested on CERTS and 38-bus microgrids system and results obtained are compared with other methods.

The reminder of this paper is organized as follows. 'Microgrid and VAI modeling' below provides the overviews of the microgrid and VAI modeling. 'Problem formulation' describes the mathematical formulation of MR problem. The introduction of SVAPO and its application in MR problem are explained in 'Overviews of SVAPO algorithm'. 'Case study and results' presents the test results and 'Conclusions' outlines the conclusion.

Microgrid and VAI modeling

A microgrid which contains a number of DGs of multiple energy forms can provide heat or cool energy for users. It operates under the islanded or grid-connected mode through the PCC switch. The traditional researches have concentrated on the model of transmission network, in which the line resistance is much smaller than the line reactance because of the high voltage level. However, the voltage level is low in distributed network, especially in a microgrid, which is only several hundred volt. So the line characteristic in a microgrid is different. Due to the high R/X ratio in a microgrid, the traditional mathematical model proposed is not available under this condition of $X \gg R$ used in the transmission network. So it is necessary to establish a novel model considering the characteristics of the microgrid, in which the line resistance cannot be ignored now.

DG Modeling

Different from traditional generators, the DG units with power electronic converters and filtering devices connect into the microgrid with some control strategies [20]. Fig. 1 depicts the equivalent circuit.

$$P = (EV/Z\cos\phi - V^2/Z)\cos\theta + EV/Z\sin\phi\sin\theta \tag{1}$$

$$Q = (EV/Z\cos\phi - V^2/Z)\sin\theta - EV/Z\sin\phi\cos\theta \tag{2}$$

Because the system impedance is resistive and ϕ is always so small, this paper assumes $Z = R$, $\theta = 0°$, $\cos\phi = 1$, $\sin\phi = \phi$. So the active and reactive powers can be decoupled. Fig. 2 illustrates the behaviors of P/Q in the polar plot [21].

From Fig. 2, the delivered active and reactive powers increase with E. But the reactive power increase with ϕ in the polar plot, whereas the active power remains constant.

Under the grid-connected mode, the large power grid can be treated as the slack bus, DGs can be equivalent to PQ, PV, and PI bus. Under the islanded mode, there is no slack bus now, each DG operates by droop strategies. Here the DGs' model under the islanded mode is built below. So the output power of DGs can be controlled by

$$P_{G_i} = \left(V_i^* - |V_i|\right)/m_{pi} \tag{3}$$

$$Q_{Gi} = (\omega^* - \omega_i)/n_{qi} \tag{4}$$

Load modeling

There are various forms of loads in a microgrid, i.e., industrial loads, commercial loads and residential loads. The voltage dependency of load characteristics can be modeled by the static load models expressed as [22]

$$P_{Li} = P_{Oi}|V_i|^{\alpha} \tag{5}$$

$$Q_{Li} = Q_{Oi}|V_i|^{\beta} \tag{6}$$

Power flow calculation

Correct power flow equations are the basis of operation and reconfiguration under either operational mode [23–25].

Under the grid-connected mode, the large power grid can be treated as the slack bus. If under the islanded mode, there is no slack bus in the system now. The system frequency plays a role as a communication medium between the different DG units. DGs with the control strategy adjust their output power to ensure the normal operation of microgrids [8].

Substituting with (7) and (9) in (8), the calculated active and reactive power for phase a can be given as in (10), (11). Similar equations can be extracted for phase b and c. The power flow equations can be expressed from (7)–(15):

$$\left[I_{ij}^{abc}\right] = \left[Y_{ij}^{abc}\right]\left[V_{ij}^{abc}\right] \tag{7}$$

$$\left[S_i^{abc}\right] = \left[V_i^{abc}\right]\left[I_{i,inj}^{abc}\right]^* \tag{8}$$

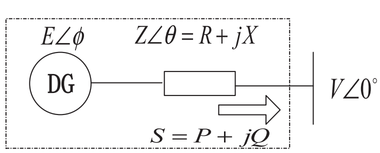

Fig. 1. Equivalent circuit of a microsource.

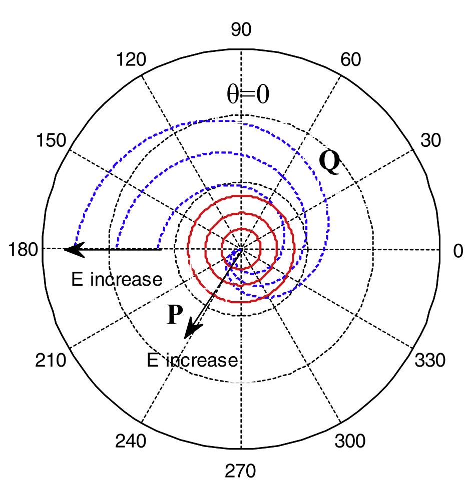

Fig. 2. Polar plot of the P/Q behaviors.

$$I_{i,inj}^{abc} = \sum_{\substack{j=1\\ j\neq i}}^{nb} I_{ij}^{abc} \tag{9}$$

$$\begin{aligned} P_i^a = \sum_{\substack{j=1\\ j\neq i}}^{nb} \sum_{ph=a,b,c} \Big[& V_i^a |Y_{ij}^{a(ph)-n}| V_i^{(ph)} \cos\left(\theta_{ij}^{a(ph)} + \phi_i^{(ph)} - \phi_i^a\right) \\ & - |V_i^a||Y_{ij}^{a(ph)-n}| V_j^{(ph)} \cos\left(\theta_{ij}^{a(ph)} + \phi_j^{(ph)} - \phi_i^a\right)\Big] \end{aligned} \tag{10}$$

$$\begin{aligned} Q_i^a = \sum_{\substack{j=1\\ j\neq i}}^{nb} \sum_{ph=a,b,c} \Big[& V_i^a |Y_{ij}^{a(ph)-n}| V_i^{(ph)} \sin\left(\theta_{ij}^{a(ph)} + \phi_j^{(ph)} - \phi_i^a\right) \\ & - |V_i^a||Y_{ij}^{a(ph)-n}| V_i^{(ph)} \sin\left(\theta_{ij}^{a(ph)} + \phi_i^{(ph)} - \phi_i^a\right)\Big] \end{aligned} \tag{11}$$

$$0 = P_{Li}^{abc} - P_{Gi}^{abc} + P_i^{abc}\left(\omega, V_i^{abc}, V_j^{abc}, \phi_i^{abc}, \phi_j^{abc}\right) \tag{12}$$

$$0 = Q_{Li}^{abc} - Q_{Gi}^{abc} + P_i^{abc}\left(\omega, V_i^{abc}, V_j^{abc}, \phi_i^{abc}, \phi_j^{abc}\right) \tag{13}$$

$$0 = P_{Gi}^a + P_{Gi}^b + P_{Gi}^c - P_{Gi}\left(V_i^{abc}\right) \tag{14}$$

$$0 = Q_{Gi}^a + Q_{Gi}^b + Q_{Gi}^c - Q_{Gi}(\omega) \tag{15}$$

Vulnerability index of structure parameters

The principle of the network topology can be described as follows: nodes stand for generators, loads and substations, and edges stand for lines. R_i is introduced to be the weighted factor. The shortest path is defined as the minimum sum path between a generator and a node, which can be expressed as:

$$Min\sum_{i\in L} R_i \tag{16}$$

Choose betweenness B and γ_{os} to express the vulnerability indices of structure parameters. Among them, the between-ness of nodes and lines B_i can be presented as the minimum sum of the shortest path going through node i or line i.

γ_{os} of element i can be defined as the ratio of the time out of operation t_{os} and total time T_s, which can be expressed as:

$$\gamma_{os} = t_{os}/T_s \tag{17}$$

The reason for choosing γ_{os} as the vulnerability index is that γ_{os} is proportional to the vulnerability.

Vulnerability index of operation state

The operation vulnerability of a microgrid is described as the ability to maintain the stability of network structure when one element or some elements are out of operation. This paper chooses bus voltage quality index-*DI*, line flow index-*OL*, and system frequency-*Sf* as operation vulnerability indices.

DI index

A microgrid aims at providing diverse power quality for users. Different kinds of bus have different power quality demand, especially the sensitive loads. For bus voltage, the *DI* is

$$DI_i = \left(|V_i| - |V_i^{sp}|\right)/\Delta V_i^{\lim} \tag{18}$$

OL index

The microgrid is designed based on the concept of the system energy demand. Line flow index is used to guarantee the energy transmission in case of the disturbance or fault. The *OL* index is:

$$OL_i = p_{li}/p_{li}^{\lim} \tag{19}$$

Sf index

Different from the distribution power system, these two operation modes are the main feature for a microgrid. The system frequency will have an impact on the power quality of sensitive loads under the grid-connected mode, however, under the islanded mode, the system frequency will be the essential condition for microgrid connecting to the large power grid again. So take the ratio of system frequency and the active power shortage as the performance index – $sfi = \partial f_i/\partial p_i$, and consider $sevf_i$ as a weighted factor of *sfi*.

$$sevf_i = \begin{cases} (49.9 - f_i)/49.9 & f_i \le 49.9\ \text{Hz} \\ 0 & 49.9\ \text{Hz} \le f_i \le 50.1\ \text{Hz} \\ (f_i - 50.1)/50.1 & f_i \ge 50.1\ \text{Hz} \end{cases} \tag{20}$$

For the system frequency, the *Sf* index is:

$$S_{fi} = \partial f_i/\partial p_i \cdot sevfi \tag{21}$$

Vulnerability assessment system

Fig. 3 illustrates the vulnerability assessment system of a microgrid. Define the whole vulnerability value of a microgrid as the product of V_o with V_s. Moreover, V_o can be expressed as the weighted sum of each operation index, and V_s can be described as the product of each structure index.

Additionally, the ISV_i and *ISV* can be expressed in the following, respectively:

$$ISV_i = V_s \cdot V_o = B_i\gamma_{os} \cdot (w_1DI_i + w_2S_{fi} + w_3OL_i) \tag{22}$$

$$ISV = \sum_{i=1}^{NB,NL} ISV_i \tag{23}$$

where, the weighting factors are calculated by the hierarchy judgment matrix listed below (Table 1).

$$F_i = \sqrt[3]{b_{i,1} \cdot b_{i,2} \cdot b_{i,3}} \quad i = 1,2,3 \tag{24}$$

$$\sum F = F_1 + F_2 + F_3 \tag{25}$$

$$w_i = F_i/\sum F \quad i = 1,2,3 \tag{26}$$

3. Problem formulation

In general, reconfiguration problem is certainly a mixed integer nonlinear optimization problem to find a best configuration of radial network [26,27]. Therefore, the MR model in this paper is built based on the vulnerability assessment system. The objective function of the problem is formulated to minimize the vulnerability value reduction in a microgrid, which is given by

Table 1
Hierarchy judgment matrix.

V_o	DI_i	S_{fi}	OL_i	w
DI_i	b_{11}	b_{12}	b_{13}	w_1
S_{fi}	b_{21}	b_{22}	b_{23}	w_2
OL_i	b_{31}	b_{32}	b_{33}	w_3

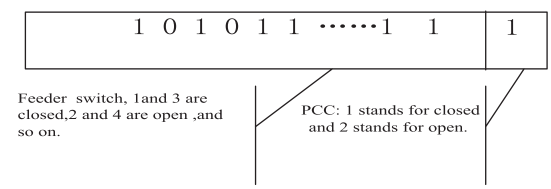

Fig. 4. Consist of individual solutions.

$$Min \quad ISV = f(X_i, X_{PCC})$$

$$ISV = \sum B_i\gamma_{os}(w_1DI_i + w_2S_{fi} + w_3OL_i) \tag{27}$$

Subject to

(a) Microgrid power flow equation

$$AP = D \tag{28}$$

(b) VAI limits

$$[DI_i, OL_i, Sf] \in V_o^{sp} \tag{29}$$

(c) Radial structure of microgrid

$$g_k \in G_k \tag{30}$$

(d) Limit of switching numbers

$$N \le N_{\max} \tag{31}$$

The objective function aims at the minimal vulnerability value of the microgrid by changing the status of feeder switches and PCC. Take the constraints about power flow and vulnerability indices into consideration to ensure the convergence of power flow and limit the VAI value. In addition, the electrical network should be radial configuration in the case of the final solution. Finally, in case of switching frequently, the constraints about operation number of switches must be limited.

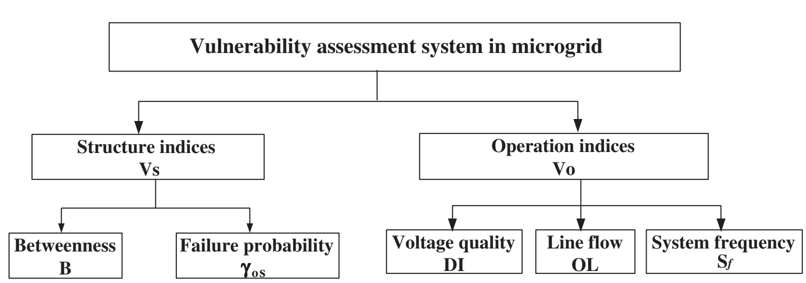

Fig. 3. Vulnerability assessment system of microgrids.

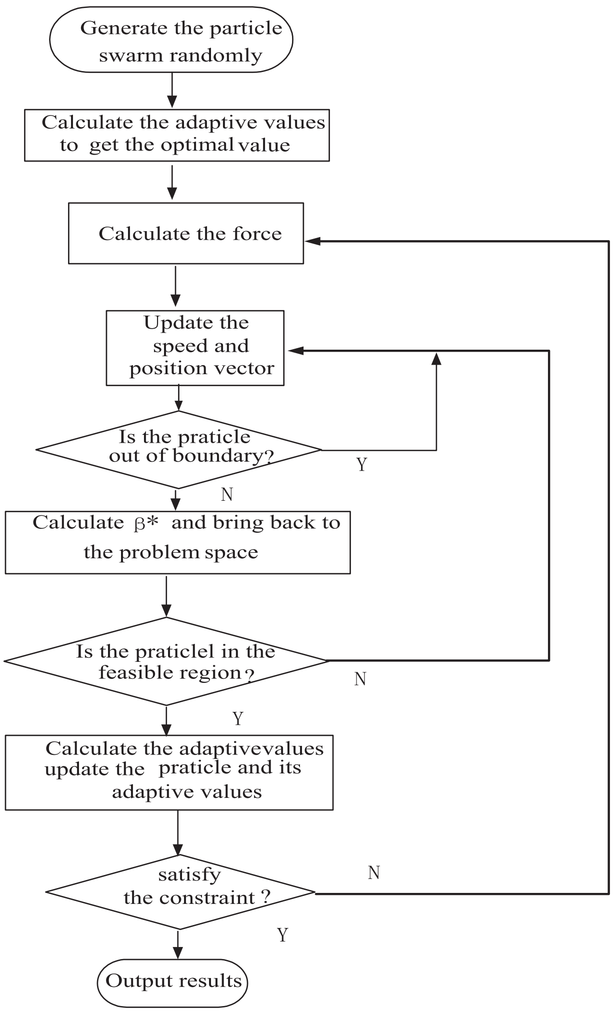

Fig. 5. Flow chart.

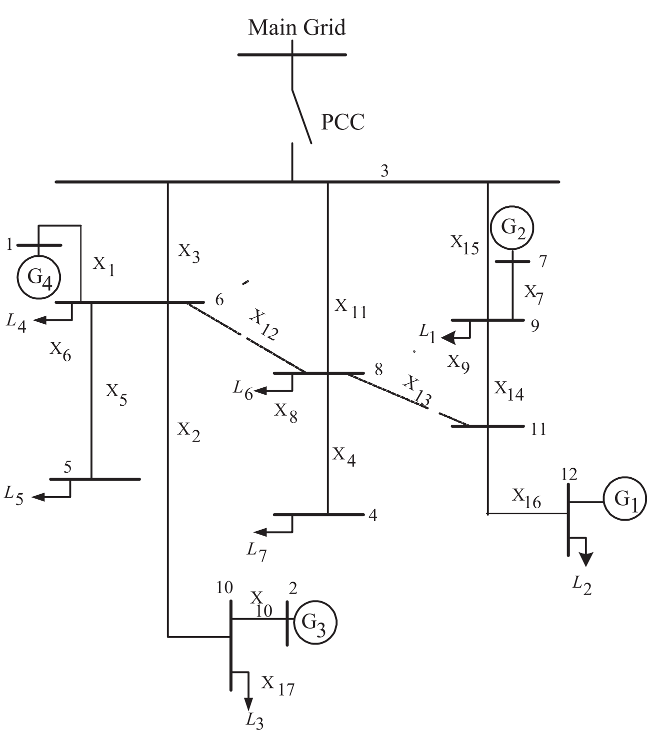

Fig. 6. Structure of CERTS.

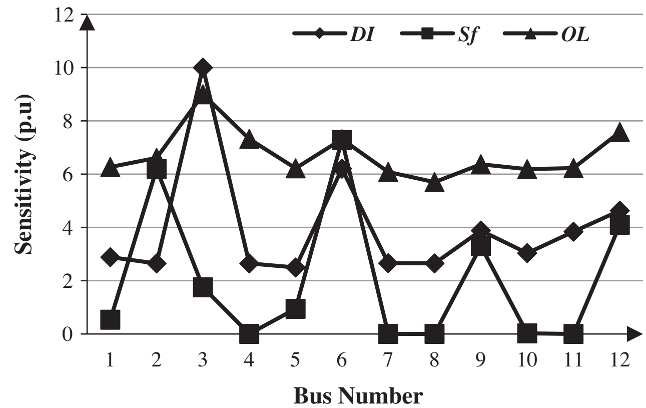

Fig. 7. Comprehensive sensitivity of nodes.

Overviews of SVAPO algorithm

The SVAPO is a new powerful population search algorithm derived from Newton's second law due to its excellent convergence characteristics. Every individual is one of the feasible solutions among the population members, which adjusts their movement by the inertia and the force from other individuals. The one-dimensional search vector is contributed to guide the searching movement in case of the local minimal. The global optimal solution is defined as the best position which the searching group has been experienced. The fitness function is developed to evaluate the quality of solutions. The individual updates the mass continuously. However, as the mass varies, the force will vary in order to update the speed and position of individuals. The main steps of SVAPO are as follows [28,29]:

Step (1) Initialize the individual initial parameters.
Step (2) Calculate the individual mass and force.

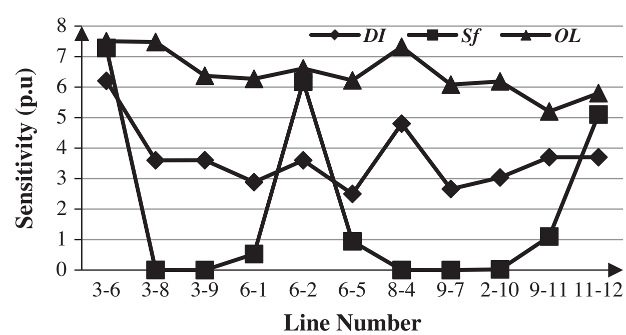

Fig. 8. Comprehensive sensitivity of feeder.

Table 2
Betweenness and fault probability.

Bus	1	2	3	4	5
Betweenness	18	51	113	35	18
γ_{os}	0.004	0.003	0.002	0.003	0.003
Bus	6	7	8	9	10
Betweenness	102	18	65	99	18
γ_{os}	0.002	0.003	0.003	0.003	0.004
Feeder	3–6	3–8	3–9	6–1	6–2
Betweenness	84	60	84	18	48
γ_{os}	0.005	0.003	0.004	0.002	0.003
Feeder	6–5	8–4	9–7	2–10	
Betweenness	18	34	18	18	
γ_{os}	0.002	0.002	0.002	0.001	

Table 3
Vulnerability of microgrid (per-unit value: 10^{-2}).

Bus	Vulnerability		
	This paper	[7]	[10]
1	21.694	1.320	0.82
2	152.349	5.035	1.25
3	199.490	15.132	3.86
4	20.319	4.720	1.17
5	49.503	3.901	1.30
6	20.569	8.772	2.83
7	16.420	1.543	0.66
8	34.913	8.421	1.63
9	98.348	10.187	3.11
10	18.652	1.113	0.50
11	51.011	2.891	0.98
12	124.692	8.273	2.89
Feeder			
	This paper	[7]	[10]
3–6	247.609	12.117	3.57
3–8	36.221	9.457	2.72
3–9	49.270	18.030	3.92
6–1	8.622	2.891	2.02
6–2	88.096	11.982	3.61
6–5	9.372	2.314	2.13
8–4	8.975	4.540	2.30
9–7	6.072	7.201	2.42
2–10	4.215	3.889	2.27
9–11	28.395	9.782	2.76
11–12	128.365	10.031	2.87

Table 4
Results of reconfiguration.

Method	Case	Scheme	PCC	*ISV*	Iteration
SV-APO	Fault	×3, ×4, ×12, ×16	0	57.23	28
GA	Fault	×3, ×5, ×12, ×16	0	58.03	73
SV-APO	Power quality	×13, ×15 L5 = 0.188	1	21.43	13
GA	Power quality	×13, ×15 L5 = 0.188	1	21.43	62

Step (3) Initialize the individual movement.
Step (4) Compute the shrinkage factor and update the individual.
Step (5) Check the termination criterion.

These steps are described in the next five subsections.

Initialize the parameters

At first, initialize the individual to get the position and speed vectors randomly in N-dimensional space. Then the optimal adaptive value of each individual is marked as x_{best} Fig. 4 depicts the composition of each individual. The left part shows the status of feeder switches, and the right part shows the status of PCC. The individual mass should be calculated before the force brings on.

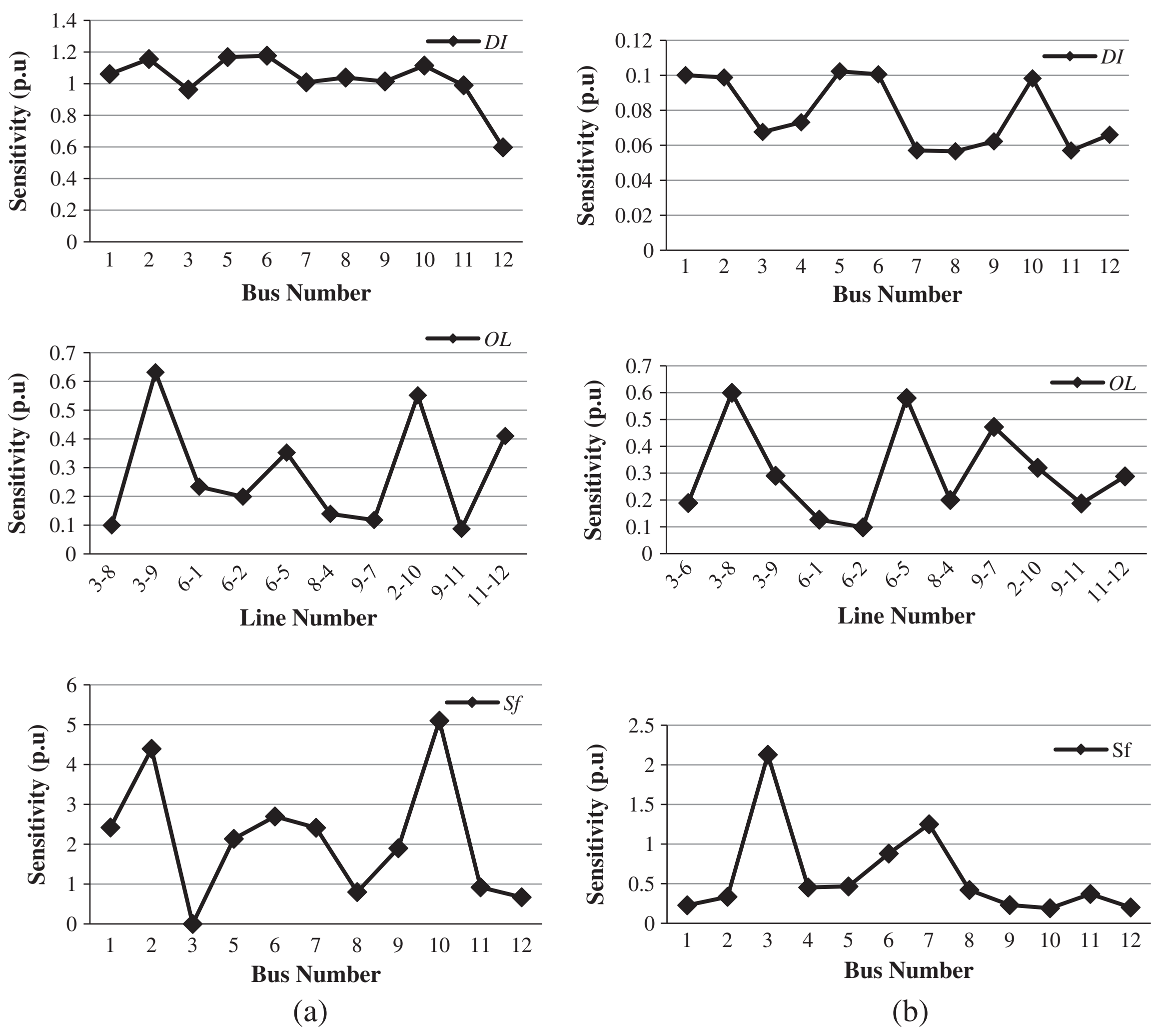

Fig. 9. Vulnerability of each operation index in each case.

Calculate the mass and force

The particle mass should be calculated before the force press on the individual.

$$m_i = e^{[f(x_{best})-f(x_i)]/[f(x_{worst})-f(x_{best})]} \tag{32}$$

Define $G_i = \{x_j | f(x_j < F(x_i), \forall x_j \in A\}$ and $W_i = \{x_j | f(x_j \geqslant F(x_i), \forall . x_j \in A\}$ as two sets respectively, in which the individual is better and worse than ith individual. In addition, the distance between ith individual and jth individual can be written as $\|x_j - x_i\| = \sqrt{\sum_{k=1}^{n}(x_{j,k} - x_{i,k})^2}$. The direction vector $\vec{r}_{ij}$ from jth individual to ith individual is specified as

$$\vec{r}_{ij} = [r_{ij,1}, r_{ij,2} \cdots r_{ij,n}] = \begin{cases} 1 & \text{if } x_{j,k} > x_{i,k} \\ 0 & \text{if } x_{j,k} = x_{i,k} \\ -1 & \text{if } x_{j,k} < x_{i,k} \end{cases} \tag{33}$$

The force bringing on ith individual from jth individual can be computed as

$$\vec{F}_{ij} = \begin{bmatrix} F_{ij,1} \\ F_{ij,2} \\ \cdots \\ F_{ij,n} \end{bmatrix} = \begin{cases} Gm_i m_j \|x_j - x_i\| \vec{r}_{ij} & x_j \in G_i \\ -Gm_i m_j \|x_j - x_i\| \vec{r}_{ij} & x_j \in W_i \end{cases} \tag{34}$$

Initialize the individual movement

The iterative equations of the speed and position vectors of individual i in kth dimension are listed in the following:

$$v_{i,k}(t+1) = w v_{i,k}(t) + \lambda F_{i,k}/m_i \tag{35}$$

$$x_{i,k}(t+1) = x_{i,k}(t) + v_{i,k}(t+1) \tag{36}$$

Compute the shrinkage factor and update the individual

Furthermore, in case of boundary violation for individual, a simplified method is described below

$$x_{i,k} = \begin{cases} x_k^u & \text{if } x_{i,k} > x_k^u \\ x_k^l & \text{if } x_{i,k} < x_k^l \end{cases} \tag{37}$$

To keep the direction of the individual, β^* is adopted to bring the solution out of boundary back to the solution space.

$$\beta_k = \begin{cases} [x_k^u - x_{i,k}(t)]/[x_{i,k}(t+1) - x_{i,k}(t)] & \text{if } x_{i,k}(t+1) > x_k^u \\ [x_k^l - x_{i,k}(t)]/[x_{i,k}(t+1) - x_{i,k}(t)] & \text{if } x_{i,k}(t+1) < x_k^l \end{cases} \tag{38}$$

Therefore, use the minimal contraction coefficient β^* to bring the position vector x_i back to the problem space.

$$\beta^* = \min\{\beta_k\} \ \beta^* \in (0, 1] \tag{39}$$

The final iterative equations of the position vectors is expressed as

$$x_{i,k}(t+1) = x_{i,k}(t) + \beta^* v_{i,k}(t+1) \tag{40}$$

However, when it is hard to make sure all the individual feasible, a one-dimensional searching method is presented to help find the solution in the direction of speed vectors, and the violation constraint function $\varphi(x)$ is suggested to check the feasibility. If the individual moves out of the solution space, a factor α (shown in (40)) regarded as the step length is used to the iterative equations to ensure the minimum constraints violation.

$$x_i(t+1) = x_i(t) + \alpha v_i(t+1), \alpha \in [0, \beta^*) \tag{41}$$

$$\min_{\alpha \in [0,\beta*)} \phi(x_i(t+1)) = \min_{\alpha \in [0,\beta*)} \phi((t) + \alpha V_i(t+1)) \tag{42}$$

Check the termination criterion

The SVAPO is terminated when the criterion has been satisfied. Otherwise, step 2 and step 3 are repeated.

The flow chart is illustrated in Fig. 5.

Case study and results

In order to demonstrate the effectiveness of the proposed method using SVAPO, it is applied to two test systems including CERTS [30] and 38-bus microgrid. The simulation has been programmed in MATLAB 2009a carried on a computer with Pentium IV, core 2, 1.6 GHz, 2 GB RAM.

CERTS microgrid

The test system is CERTS microgrid with 2 tie switches, 15 sectionalizing switches and 1 PCC switch illustrated in Fig. 6. The parameters of SVAPO algorithm are $\lambda \sim U(0,1)$ and $\omega \in (0.4, 0.9)$.

This paper has assumed that the microgrid is connected to the large power grid at first, that means $X_{PCC} = 1$, and the large power grid transmits power energy to the microgrid. The structure parameters of the CERTS are listed in Table 2. The vulnerability indices of operation status are illustrated from Figs. 7 and 8.

According to Table 2, Figs. 7 and 8, substitute with the data above in (22) to get the vulnerability value of the microgrid described in Table 3.

From Table 3, the importance of loads is different, so is the vulnerability value of buses and lines. However, the vulnerability value of sensitive loads (L1, L2) is high, which reflects the main

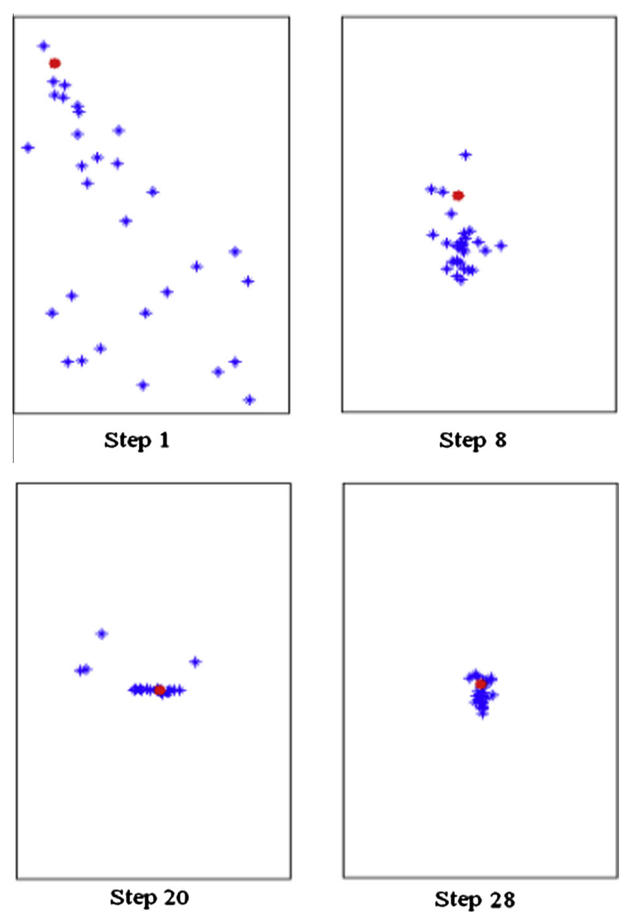

Fig. 10. The optimization process of SV-APO algorithm in fault.

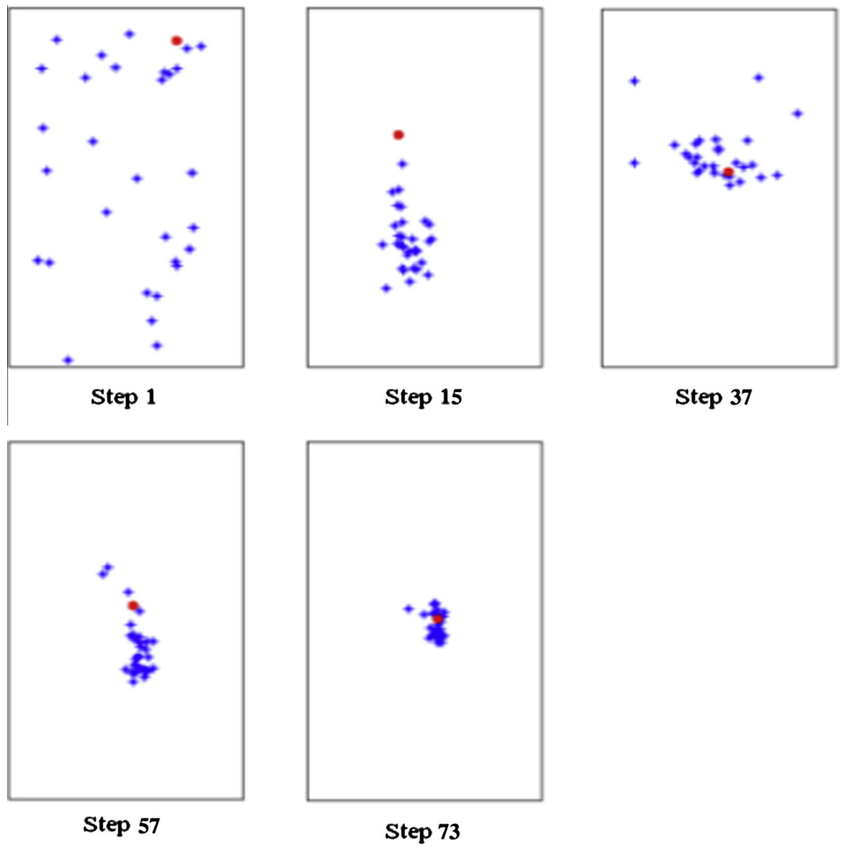

Fig. 11. The optimization process of GA algorithm in fault.

feature of a microgrid—the voltage quality and the power energy transmission management. In addition, two other different methods explained in reference have been chosen to compare the performance of the method proposed in this paper. The results verify the correctness of the proposed method in this paper.

Consider the power grid fault and the decline of power quality of sensitive loads, respectively. Table 4 shows the reconfiguration results. Fig. 9(a and b) illustrate the operation VAI in each case. And the comparison of iteration convergence of algorithm is presented in Figs. 10 and 11.

From Table 4 and Fig. 9(a and b), the vulnerability of each operation index varies with the different disturbances Therefore, it is necessary to adopt different dispatching modes. When the fault happened, the microgrid should immediately switch to the islanded operation mode according to the analysis of the vulnerability assessment system. Then, islanded reconfiguration of CERTS microgrid can not only supply the power shortage, but also ensure the high power quality for sensitive loads (L2 has been isolated from the rest system) by shedding a number of interruptible loads.

When the decline of the power quality of L1 happened, it is necessary to adjust the control strategy right now according to operation principle of a microgrid. Whereas, the reconfiguration scheme under the grid-connected mode is able to meet the power quality of sensitive loads, there is no need to open PCC switch so that the operation cost and difficulties are reduced. The reconfiguration scheme aims at minimizing the vulnerability value of a microgrid as well as satisfying the constraints to prevent the occurrence of cascading failure. Moreover, from Figs. 10 and 11, the convergence of SV-APO algorithm put forward in this paper is faster than the GA algorithm, especially in complicated calculation In the process of iteration, the GA algorithm is easy to be local convergence. On the contrary, the SV-APO algorithm can get the global optimal solution quickly and accurately which will provide a strong technical support to the research in the future.

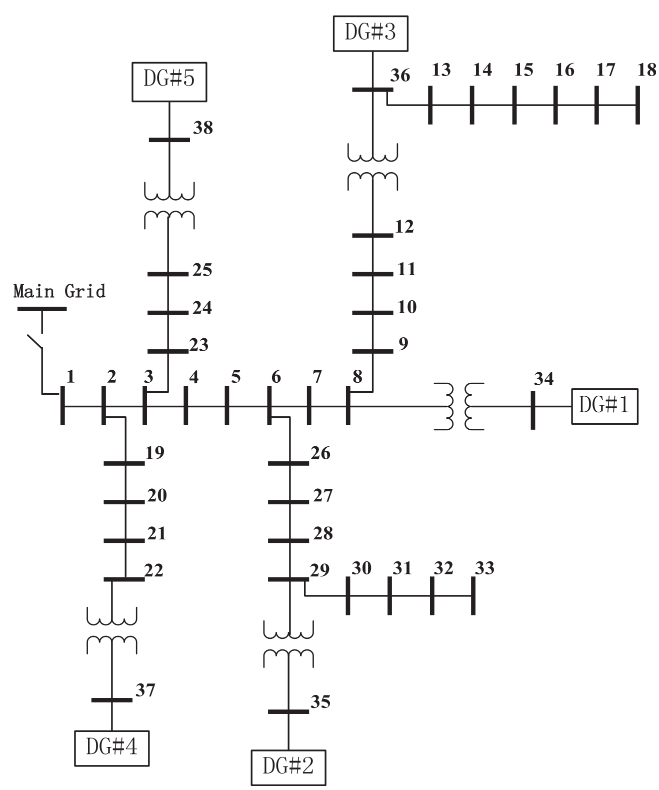

Fig. 12. 38-Bus microgrid system.

Table 5
Vulnerability of typical buses.

Bus	Vulnerability	Feeder	Vulnerability
3	65.701	3–28	31.603
4	45.315	3–36	41.102
8	32.393	4–47	33.794
9	34.663	8–68	24.527
11	12.276	9–55	12.166
12	21.125	11–53	20.305
5	4.458	12–51	3.073
12	24.093	18–19	12.711
28	11.715	24–25	7.776
36	8.256	40–41	4.206
47	13.987	44–45	9.269
53	6.963	59–60	3.769
55	10.492		

Table 6
Results of reconfiguration after fault.

Method	Case	Scheme	PCC	*ISV*	Iteration
[32]	Fault	6–7,14–15,32–33,18–33	1	943.220	84
[33]	Fault	11–12,13–14,30–31,25–29	1	915.403	44
APO	Fault	10–11,13–14,31–32,25–29	1	911.727	42
SV-APO	Fault	10–11,13–14,31–32,25–29	1	911.727	32

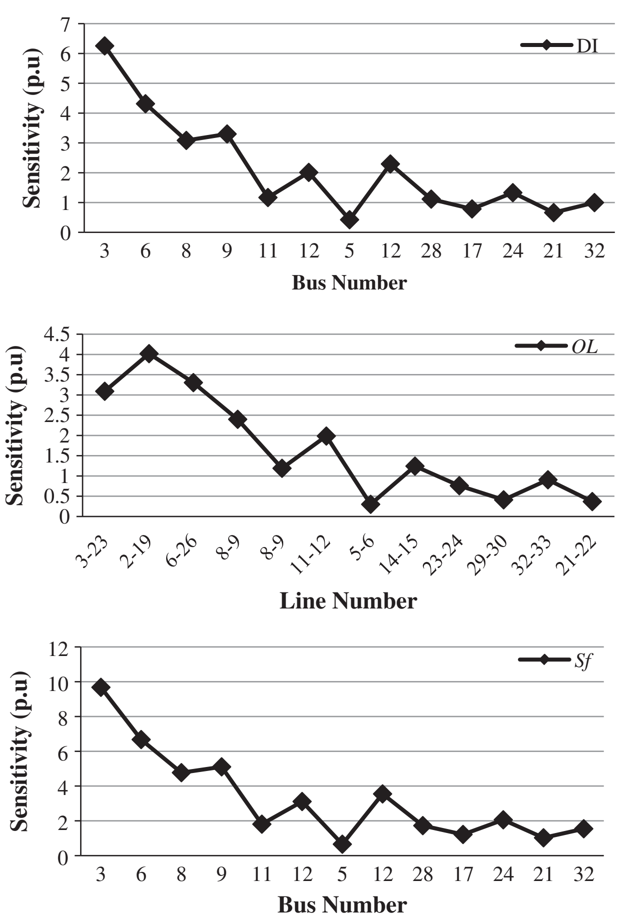

Fig. 13. Vulnerability of each operation index using SVAPO.

38-bus microgrid

Fig. 12 is a 38-bus microgrids with 5 tie switches, 32 sectionalizing switches and 1 PCC switch. Configuration, loads, lines and tie lines data are taken from [31]. The vulnerability value of typical buses and feeders is described in Table 5.

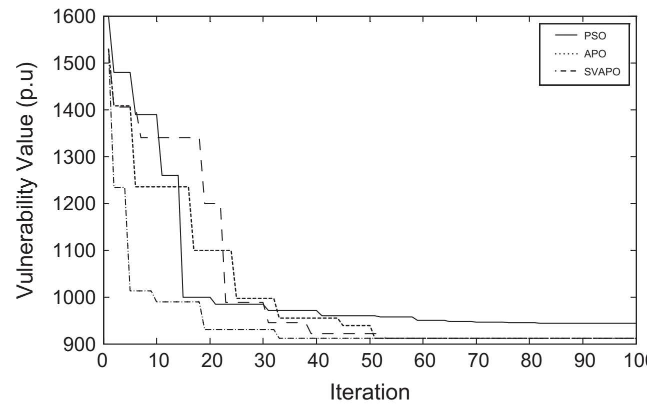

Fig. 14. Comparision of each algorithm.

Similar to CERTS system, this test system is also simulated for reconfiguration based on vulnerability assessment. The results of reconfiguration after line 2–3 fault are illustrated in Table 6. Figs. 13 and 14 show the vulnerability of each operation indices and comparison of each optimization algorithm.

From Fig. 13, it is observed that the sensitivity of buses and lines near the fault point is increasing heavily. Table 6 and Fig. 14 show the performance of the SVAPO is better than other algorithm presented in several references in terms of the quality and convergence of solutions.

Conclusions

The MR problem has been investigated using application of SVAPO algorithm based on the microgrid mathematical model and vulnerability assessment system. The vulnerability assessment system was used to present the microgrid vulnerability considering the topological parameters and operational parameters. Developed method has been tested for CERTS and 38-bus microgrids under several scenarios. The results show that the vulnerability assessment system is proposed on the foundation of structural characteristics and operation status of microgrids, which overcomes the one-sidedness of traditional assessment methods to identify weak points effectively. The results show that the MR reconfiguration problems were formulated to minimize the total vulnerability of microgrids considering the grid-connected/islanded modes. The computational results obtained using SVAPO algorithm was better than GA algorithm. The performance of SVAPO algorithm proves to provide theoretical and practical basis for subsequent engineering applications as well as a reference for maintenance and management of the power grid.

Acknowledgement

The authors would like to acknowledge the supports from National Basic Research Program of China (973 Program, 2012CB215201) for the work reported in this paper.

References

[1] Das D. A fuzzy multi-objective approach for network reconfiguration of distribution systems. IEEE Trans Power Del 2006;21(1):202–9.
[2] Wallnerström Carl Johan, PatrikHilber. Vulnerability analysis of power distribution systems for cost-effective resource allocation. IEEE Trans Power Syst; 2011.
[3] Lasseter RH, Eto JH, Schenkman B, Stevens J, Vollkommer H, Klapp D, et al. Certs microgrid laboratory test bed. IEEE Trans Power Del 2011;26(1):325–32.

[4] Lee Chia-Tse, Chu Chia-Chi, Cheng Po-Tai. A new droop control method for the autonomous operation of distributed energy resource interface converters. IEEE Trans Power Electron 2013;28(4):1980–93.
[5] Rowe Christopher N, Summers Terrence J, Betz Robert E, Cornforth David J, Moore Timothy G. Arctan power–frequency droop for improved microgrid stability. IEEE Trans Power Electron 2013;28(8):3747–59.
[6] Babazadeh Maryam, Karimi Houshang. A robust two-degree-of-freedom control strategy for an islanded microgrid. IEEE Trans Power Del 2013;28(3): 1–9.
[7] Wang Ansi, Luo Yi, Guangyu Tu, Liu Pei. Vulnerability assessment scheme for power system transmission networks based on the fault chain theory. IEEE Trans Power Syst 2011;26(1):442–50.
[8] Ten Chee-Wooi, Liu Chen-Ching, Manimaran Govindarasu. vulnerability assessment of cybersecurity for SCADA systems. IEEE Trans Power Syst 2008;23(4):1836–46.
[9] Carrión Miguel, Arroyo José Manuel, Alguacil Natalia. Vulnerability-constrained transmission expansion planning: a stochastic programming approach. IEEE Trans Power Syst 2007;22(4):1436–45.
[10] Xingbin Yu, Singh Chanan. A practical approach for integrated power system vulnerability analysis with protection failures. IEEE Trans Power Syst 2004;19(4):1811–20.
[11] Overbye Thomas J, DeMarco Christopher L. An energy based security measure for assessing vulnerability to voltage collapse. IEEE Trans Power Syst 1990; 5(2):419–27.
[12] A Fouad A, Zhou Qin, Vitta1 V. System vulnerability as a concept to assess power system dynamic security. IEEE Trans Power Syst 1994;9(2). V1009-15.
[13] Chen Xiao-gang, Sun Ke, Cao Yi-jia. Structural vulnerability analysis of large power grid based on complex network theory. Trans China Electro Tech Soc 2007;22(10):138–44.
[14] Ying Shao, Ji-lai Yu. Power grid vulnerability assessment based on electrical dissection information of the electric power network. Proc CSEE 2009;29(31): 34–9.
[15] González Alezeia, Echavarren Francisco M, Rouco Luis, Gómez Tomás. A sensitivities computation method for reconfiguration of radial networks. IEEE Trans Power Syst 2012.
[16] Srinivasa Rao R, Ravindra K, Satish K, Narasimham SVL. Power loss minimization in distribution system using network reconfiguration in the presence of distributed generation. IEEE Trans Power Syst 2013.
[17] Zin Abdullah Asuhaimi Mohd, Ferdavani Ali Khorasani, Khairuddin Azhar Bin, Naeini Marjan Mortazavi. Reconfiguration of radial electrical distribution network through minimum-current circular-updating-mechanism method. IEEE Trans Power Syst 2012;27(2):968–74.
[18] Reza Malekpour Ahmad, Niknam Taher, Pahwa Anil, Fard Abdollah Kavousi. Multi-objective stochastic distribution feeder reconfiguration in systems with wind power generators and fuel cells using the point estimate method. IEEE Trans Power Syst 2013;28(2):1483–92.
[19] Zin Abdullah Asuhaimi Mohd, Ferdavani Ali K, Khairuddin Azhar Bin, Naeini Marjan M. Two circular-updating hybrid heuristic methods for minimum-loss reconfiguration of electrical distribution network. IEEE Trans Power Syst 2013;28(2):1318–23.
[20] Abdelmageed Abdelaziz Morad Mohamed, Farag Hany E, El-Saadany Ehab F, Mohamed Yasser Abdel-Rady I. A novel and generalized three-phase power flow algorithm for islanded microgrids using a Newton trust region method. IEEE Trans Power Syst 2012.
[21] Yao W, Chen M, Matas J, Guerrero JM, Qian Z-M. Design and analysis of the droop control method for parallel inverters considering the impact of the complex impedance on the power sharing. IEEE Trans Ind Electron 2011;58(2): 576–88.
[22] Szuvovivski I, Fernandes TSP, Aoki AR. Simultaneous allocation of capacitors and voltage regulators at distribution networks using genetic algorithms and optimal power flow. Int J Elect Power Energy Syst 2012;40(1):62–9.
[23] De Oliveira Leonardo W, Carneiro Jr Sandoval, de Oliveira Edimar J, Pereira JLR, Silva Jr Ivo C, Costa Jeferson S. Optimal reconfiguration and capacitor allocation in radial distribution systems for energy losses minimization. Int J Electr Power Energy Syst 2010;32(8):840–8.
[24] Gonzalez A, Echavarren FM, Rouco L, Gomez T, Cabetas J. Reconfiguration of large scale distribution networks for planning studies. Int J Elect Power Energy Syst 2012;37(1):86–94.
[25] Raju GKV, Bijwe PR. An efficient algorithm for minimum loss reconfiguration of distribution system based on sensitivity and heuristics. IEEE Trans Power Syst 2008;23(3):1280–7.
[26] Garcia VJ, Franca P. Multiobjective service restoration in electric distribution networks using a local search based heuristic. Eur J Oper Res 2008;189(3): 649–705.
[27] Chandramohan S, Atturulu N, Kumudini RP, Ventakesh B. Operating cost minimization of a radial distribution system in a deregulated electricity market through reconfiguration using NSGA method. Int J Electr Power Energy Syst 2010;32(2):126–32.
[28] Qiao Y, Lu Z, Mei S. Microgrid reconfiguration in catastrop failure of large power systems. In: Intl conf sustainable power generation and supply, Nanjing; 2009.
[29] Singh D, Misra RK, Singh D. Effect of load models in distributed generation planning. IEEE Trans Power Syst 2007;22(4):2204–12.
[30] Mohammadi M, Hosseinian b SH, Gharehpetian GB. GA-based optimal sizing of microgrid and DG units under pool and hybrid electricity markets. Int J Electr Power Energy Syst 2012;35:83–92.
[31] Moradi Mohammad H, Eskandari Mohsen, Showkati Hemen. A hybrid method for simultaneous optimization of DG capacity and operational strategy in microgrids utilizing renewable energy resources. Int J Electr Power Energy Syst 2014;56:241–58.